

See discussions, stats, and author profiles for this publication at: <https://www.researchgate.net/publication/5636759>

# Separation of Different Hydrogen-Bonded Clusters by Femtosecond UV-Ionization-Detected Infrared Spectroscopy: 1 H - Pyrrolo[3,2- h ]quinoline·(H<sub>2</sub>O)<sub>n</sub> =1,2 Complexes

ARTICLE in THE JOURNAL OF PHYSICAL CHEMISTRY A · MARCH 2008

Impact Factor: 2.69 · DOI: 10.1021/jp076839j · Source: PubMed

CITATIONS

24

READS

31

8 AUTHORS, INCLUDING:



**Maksim Kunitski**

Goethe-Universität Frankfurt am Main

37 PUBLICATIONS 350 CITATIONS

SEE PROFILE



**Alexander Kyrychenko**

V. N. Karazin Kharkiv National University

66 PUBLICATIONS 886 CITATIONS

SEE PROFILE



**Jerzy Herbich**

Instytut Chemii Fizycznej PAN

46 PUBLICATIONS 1,100 CITATIONS

SEE PROFILE



**J. Waluk**

Polish Academy of Sciences

257 PUBLICATIONS 3,706 CITATIONS

SEE PROFILE

# Separation of Different Hydrogen-Bonded Clusters by Femtosecond UV-Ionization-Detected Infrared Spectroscopy: 1*H*-Pyrrolo[3,2-*h*]quinoline·(H<sub>2</sub>O)<sub>*n*</sub>=1,2 Complexes

Yevgeniy Nosenko,<sup>†,‡</sup> Maksim Kunitski,<sup>†</sup> Christoph Riehn,<sup>§</sup> Randolph P. Thummel,<sup>||</sup> Alexander Kyrychenko,<sup>‡</sup> Jerzy Herbich,<sup>‡</sup> Jacek Waluk,<sup>‡</sup> and Bernhard Brutschy\*,<sup>†</sup>

*Institute of Physical and Theoretical Chemistry, University of Frankfurt, Max-von-Laue-Str. 7, 60438 Frankfurt/M, Germany; Institute of Physical Chemistry, Polish Academy of Sciences, Kasprzaka 44, 01-224 Warsaw, Poland; Department of Chemistry, Technical University of Kaiserslautern, Erwin-Schrödinger-Str. 52, 67663 Kaiserslautern, Germany; and Department of Chemistry, University of Houston, Houston, Texas 77204-5003*

Received: August 27, 2007; In Final Form: November 14, 2007

Experimental and theoretical studies are presented for complexes of water with 1*H*-pyrrolo[3,2-*h*]quinoline (PQ), a bifunctional compound acting simultaneously as a hydrogen-bond donor and acceptor. A 1:1 complex, which is not fluorescent and only very short-lived in the electronically excited state, was analyzed by isolating the complex under supersonic jet conditions and characterizing its structure by infrared-induced ion depletion spectroscopy utilizing multiphoton ionization by femtosecond UV pulses (IR/fsMPI spectroscopy). On the other hand, a long-lived 1:2 complex was identified as the smallest microhydrate of PQ contributing to the laser-induced fluorescence excitation spectrum. Its structure was assigned by fluorescence-detected IR spectra and analyzed using density functional theory. The structures of the 1:1 and 1:2 clusters are assigned to species in which the water molecule(s) form a hydrogen-bonded solvent bridge between the two functional groups. In accord with calculations, both 1:1 and 1:2 PQ/water complexes reveal weaker hydrogen bonding than the analogous clusters of PQ with methanol.

## 1. Introduction

A fast phototautomerization process has been demonstrated for 1*H*-pyrrolo[3,2-*h*]quinoline (PQ) in protic solvents.<sup>1–3</sup> PQ represents a family of bifunctional molecules which possess both a hydrogen-bond donor (e.g., an aromatic NH group) and an acceptor (e.g., a quinoline-type nitrogen atom N<sub>Q</sub>). In alcohols<sup>1,2</sup> and water,<sup>3</sup> PQ shows dual luminescence, contrary to its behavior in nonpolar and polar aprotic solvents. In order to prove that the appearance of a low-energy emission band is a manifestation of an excited-state proton transfer (ESPT) process, the spectral position of this fluorescence has been compared with the emission of a N<sub>Q</sub>-methylated molecule synthesized to serve as a chemical model of the tautomeric structure.<sup>1</sup> The driving force for ESPT is provided by large p*K*<sub>a</sub> changes upon photoexcitation. For PQ, the quinoline nitrogen becomes much more basic (Δp*K*<sub>a</sub> = +9.6) and the acidity of the NH group is also strongly enhanced (Δp*K*<sub>a</sub> = −6). Titration of solutions of PQ in a nonpolar solvent with alcohol (in concentrations low enough to prevent the formation of alcohol oligomers) and the observations of spectral changes both in absorption and emission gave strong evidence that the proton transfer occurs in a 1:1 hydrogen-bonded complex of an excited chromophore with an alcohol molecule. The detailed structural characterization of the reactive precursors is a challenging task for solution studies. It has been assumed that these complexes correspond to a 1:1 “correctly prepared” doubly hydrogen-bonded cyclic structure (Figure 1).<sup>1–3</sup> This idea has been corroborated by the finding

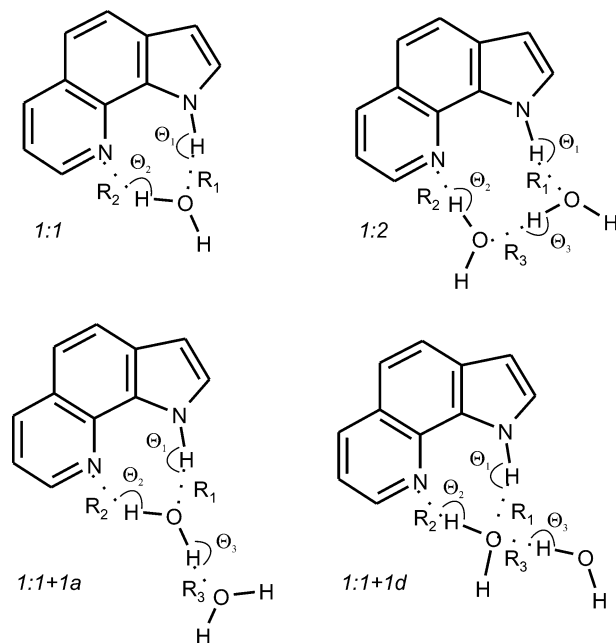


**Figure 1.** Schematic structures of the considered hydrogen-bonding complexes of PQ with water.

that the low-energy emission is still observed in glasses at temperatures as low as 77 K. Moreover, the photoreaction is extremely fast.<sup>4</sup> The decay of the primary excited fluorescence is not monoexponential and consists of a fast component (a few picoseconds) and a slow component, which increases from tens to more than a hundred picoseconds with an increase in the viscosity of the surrounding medium. Only the fast component, not much dependent on the properties of the alcohol, is observed

\* Corresponding author. E-mail: brutschy@chemie.uni-frankfurt.de.

<sup>†</sup> University of Frankfurt.

<sup>‡</sup> Polish Academy of Sciences.

<sup>§</sup> University of Kaiserslautern.

<sup>||</sup> University of Houston.

in the rise of the tautomeric fluorescence. Therefore, the general picture for the bulk solution corresponds to a dynamic equilibrium between various solvates of different stoichiometry and/or different structure.<sup>1</sup> Some of these complexes decay radiationlessly within tens or hundred picoseconds, being responsible for the viscosity-dependent fluorescence quenching. This model has also been supported by a recent time-dependent density functional theory (TDDFT) study performed for PQ/water<sub>*n*</sub> (*n* = 0,1,2) clusters.<sup>5</sup> It has been demonstrated that the barrier for the ESPT is dramatically reduced from 20.9 kcal/mol in the bare PQ molecule to 3 kcal/mol in the 1:1 PQ/water complex. Moreover, the TDDFT calculations predict that the extension of the hydrogen-bonded chain connecting the hydrogen-bond donor/acceptor groups of PQ in the 1:2 complex (Figure 1) results in an increase of the tautomerization barrier to 5.6 kcal/mol, due to unfavorable hydrogen-bond configurations. Moreover, the fraction of the 1:1 complex of PQ/water compared to PQ/methanol in solution has been estimated by a molecular dynamics (MD) simulation to be a factor of 3.5 smaller,<sup>6</sup> in agreement with the experimental value of 2.7.<sup>3</sup> Most of the previous studies focused on experiments in solution. In order to characterize the structure of these reactive hydrogen-bonded complexes with alcohols and water and to pave the way to unraveling their size-dependent chemical dynamics, we have recently started a study of the clusters isolated under supersonic jet conditions. These issues provided motivation for the present molecular beam investigations of the PQ/water<sub>*n*</sub> clusters.

We have recently shown that the photophysics of jet-isolated complexes of PQ with methanol is strongly dependent on the cluster size.<sup>7</sup> Complete lack of fluorescence, observed for the 1:1 complex, was explained by a fast ESPT reaction, that is, a phototautomerization, followed by a nonradiative relaxation of the vibrationally excited tautomer. It has been found that the fluorescence of the 1:2 PQ/methanol cluster is quenched only when the cluster is excited above the reaction barrier of about 1.9 kcal/mol. This value is an order of magnitude lower than the binding energy of the cluster, indicating the onset of a specific deactivation process. Such behavior can be correlated with the viscosity dependence of fluorescence quenching in alcohol solutions, which implies that the radiationless process involves large-amplitude motion of the alcohol molecules bonded to PQ. This motion, in turn, can be vibrationally activated. Accordingly, while for the 1:2 complex a fluorescence-detected infrared (FDIR) spectrum was readily recorded, this spectrum was not observed for the "dark" 1:1 aggregate.

A short excited state (*S*<sub>1</sub>) lifetime, as well as an ionization potential higher than twice the value of the energy of the *S*<sub>1</sub> ← *S*<sub>0</sub> transition, prevents both the detection and structural analysis of the reactive precursors by conventional double-resonance IR resonant two-photon ionization depletion spectroscopy (IR/R2PI) using nanosecond lasers.<sup>8</sup> However, by using femtosecond laser pulses for the photoionization step, we have recently demonstrated that ion depletion spectroscopy can also be successfully applied to multiphoton ionization via resonances in the continuum of excited states, with the drawback that the method is no longer isomer-specific and of limited size selectivity. This new technique was termed infrared/femtosecond multiphoton ionization spectroscopy (IR/fsMPI).<sup>9</sup> Here the third harmonic of a titanium:sapphire (Ti:Sa) laser (266 nm) was used for a resonant two-photon ionization (R2PI) of PQ and its methanol clusters via a higher singlet excited state (*S*<sub>4</sub> or *S*<sub>5</sub>) of  $\pi\pi^*$  character. By probing the ion signal of the PQ/methanol complexes by IR/fsMPI spectroscopy in the region of the hydrogen-bonded NH and OH stretch vibrations, cyclic doubly

and triply hydrogen-bonded structures were assigned, analogous to the 1:1 and 1:2 complexes depicted in Figure 1.<sup>9</sup>

In the present work we report IR/fsMPI and FDIR spectra of PQ/water<sub>*n*=1,2</sub> complexes. The structural analysis of the vibrational fingerprints is performed by means of DFT calculations.

## 2. Experimental

**2.1. Materials.** 1*H*-Pyrrolo[3,2-*h*]quinoline (PQ) was synthesized and purified according to the procedures described earlier.<sup>10</sup> Distilled water and helium of 4.6 grade were used for the preparation of PQ/water clusters under supersonic expansion conditions.

**2.2. Methods.** The details of laser-induced fluorescence (LIF) excitation and of FDIR<sup>11</sup> depletion spectroscopy have been described previously.<sup>7</sup> The FDIR and IR-UV hole-burning<sup>12</sup> spectra were measured with modification of the earlier experiment with PQ/methanol, utilizing a tunable DMQ dye laser (FL2002/LPX200, LambdaPhysik) as the UV laser source.

The experimental setup for the IR/fsMPI measurements consists of a narrow band, injection-seeded nanosecond IR optical parametric oscillator (OPO) for vibrational excitation, a femtosecond chirped-pulse amplified Ti:Sa laser system for two-photon ionization of the clusters, and a vacuum apparatus, equipped with a heated pulsed nozzle and a home-built linear time-of-flight mass spectrometer. All components have been described previously in separate publications.<sup>13,14</sup> Below, we briefly describe how these components were combined in the experiment.

The fundamental output (800 nm) of a femtosecond chirped-pulse amplified Ti:Sa laser system was frequency-tripled (efficiency 18%) resulting in laser pulses (30  $\mu$ J, 266 nm, 260 fs autocorrelation) that were used to photoionize PQ/water clusters. The femtosecond laser beam was spatially overlapped in the ionization region of the time-of-flight spectrometer with a counter-propagating nanosecond IR-OPO beam. Both laser beams crossed perpendicularly a pulsed molecular beam collimated from a seeded supersonic expansion of PQ and water with helium as the carrier gas at a stagnation pressure of 3 bar. The sample/nozzle temperature was maintained at about 380 K in order to have sufficient vapor pressure of PQ. The partial pressure of water was controlled by means of a gas mixing unit. The wavelength of the IR-OPO pulses (4 mJ, 0.2  $\text{cm}^{-1}$  fwhm, 6 ns) was scanned in the 3100–3450  $\text{cm}^{-1}$  region in order to record the IR/fsMPI depletion spectra. At each spectral point, the amplified and integrated time-of-flight signal corresponding to the selected PQ/water clusters was averaged over 40 laser shots. Finally, the spectra were averaged over up to 5 scans. The synchronization of the pulsed nozzle (General Valve, 10 Hz), IR-OPO (10 Hz), and 1 kHz femtosecond laser system was achieved with a digital delay generator (DG535, Stanford Research Systems) that was triggered by an arbitrary femtosecond laser pulse from the kHz sequence, so that after predetermined time delays, the pulsed nozzle and the IR-OPO laser were started. The nozzle delay was optimized in order to overlap in time a femtosecond laser pulse next to the trigger (1 ms later) with the molecular beam pulse in the ionization region of the mass spectrometer. The IR laser was fired 50 ns prior to the ionizing UV laser. This delay was set and checked with a photodiode. The delay generator was accepting an input trigger only every 100 ms, providing an effective repetition rate of 10 Hz.

## 3. Results

**3.1. DFT Calculations.** The geometry optimization of the 1:1 and 1:2 complexes of PQ with water in the ground and the

**TABLE 1: Ground-State Binding Energies (in kcal/mol), Selected Distances (in Å), and Angles (in degrees) of Various PQ/Water (Methanol) Complexes**

|                      | 1:1                |                   | 1:1+1                |                   |                    | 1:2                  |                      |
|----------------------|--------------------|-------------------|----------------------|-------------------|--------------------|----------------------|----------------------|
|                      | methanol           | water             | methanol             | water (1:1+1d)    | water (1:1+1a)     | methanol             | water                |
| $\Delta E(S_0)$      | -10.4 <sup>a</sup> | -9.3 <sup>b</sup> | -11.8 <sup>a,c</sup> | -9.3 <sup>c</sup> | -11.0 <sup>c</sup> | -13.9 <sup>a,c</sup> | -12.6 <sup>b,c</sup> |
| $R_1$                | 1.880              | 1.907             | 1.938                | 1.975             | 1.848              | 1.870                | 1.906                |
| $R_2$                | 1.831              | 1.816             | 1.763                | 1.740             | 1.900              | 1.798                | 1.785                |
| $R_3$                |                    |                   | 1.882                | 1.905             | 1.975              | 1.742                | 1.753                |
| $\Theta_1$           | 156.8              | 156.1             | 154.5                | 153.6             | 158.8              | 166.0                | 163.8                |
| $\Theta_2$           | 165.2              | 165.7             | 168.4                | 168.9             | 162.0              | 174.5                | 173.1                |
| $\Theta_3$           |                    |                   | 174.4                | 171.3             | 178.2              | 162.4                | 161.7                |
| $\angle \text{ONNO}$ |                    |                   |                      |                   |                    | 23.2                 | 17.7                 |

<sup>a</sup> Ref 7. <sup>b</sup> Ref 5. <sup>c</sup> The binding energy was evaluated for the interaction between PQ and a water (methanol) dimer, so that it does not include a contribution of water–water (methanol–methanol) hydrogen bonding. The energy of water–water (methanol–methanol) interaction was estimated to be -2.6 (-3.9) kcal/mol at the same level of theory.

first excited singlet states has recently been performed at the B3LYP/cc-pVDZ level of theory.<sup>5</sup> The cyclic 1:2 complex has been found to be the most stable structure among the hydrogen-bonded clusters that are possible with two water molecules. Since several stable isomers corresponding to local minima could eventually also be stabilized in the supersonic beam, we considered additionally two other isomers of the 1:2 complex. Both configurations correspond to a modified 1:1 complex, in which the second water molecule is hydrogen-bonded to the water molecule of the cyclic 1:1 cluster either as a hydrogen-bonding acceptor (1:1+1a in Figure 1) or as a donor (1:1+1d in Figure 1). The basis set superposition error (BSSE) and zero-point energy (ZPE) corrected ground-state binding energies for all relevant complexes are presented in Table 1 together with the corresponding values for structurally related PQ/methanol clusters.<sup>7</sup> Generally, the stabilization energies of the PQ/water complexes are lower by 10% than those of the PQ/methanol analogs.

Selected structural parameters (see Figure 1 for definition) of the PQ/water and PQ/methanol clusters are compared in Table 1. The hydrogen-bond length and angle values in the PQ/water clusters compared to PQ/methanol demonstrate systematically weaker hydrogen-bonding of the water bridge at the pyrrole site and a stronger one at the quinoline site. The latter can hardly be explained in terms of the relative hydrogen-bonding donor and acceptor abilities of water and methanol molecules. Apparently, the methanol complexes should be stronger in both senses as the isolated water exhibits both weaker proton affinity<sup>15</sup> and acidity<sup>16</sup> than methanol. In cyclic structures, a solvent-specific cooperativity effect comes into play as revealed by the non-additivity of hydrogen-bonding energies in the  $n = 3, 4$  clusters of water<sup>17</sup> and methanol.<sup>18</sup> Generally, small clusters of water and methanol form similar structures but the differences between them are determined by the methyl group of methanol. For the 1:2 complexes of PQ, the water bridge provides a more planar hydrogen-bonding network than the one with methanol. The characteristic ONNO dihedral angles in the ground state are 17.7 and 23.2 degrees for the water and methanol complexes, respectively. This effect may be explained by interaction between the methyl groups and the PQ molecule.

The binding energies, structures, and normal modes of the PQ/water complexes were calculated on the B3LYP/cc-pVDZ level of theory using the TURBOMOLE program package, Version 5.7,<sup>19</sup> as published previously.<sup>5</sup> Ground-state fundamental frequencies were obtained by scaling the harmonic values with a factor of 0.9704 as proposed by Witek and Morokuma.<sup>20</sup>

**3.2. LIF Excitation Spectrum.** Changes in the LIF excitation spectrum of PQ after increase of the vapor pressure of water are depicted in Figure 2a. This spectrum was measured with

the apparatus in the Warsaw Laser Centre. New spectral features corresponding to the onset of cluster formation show great similarity to those observed in the spectra with methanol. The band at 28061 cm<sup>-1</sup> is assigned to the vibrational origin of the smallest cluster of PQ with water which exhibits fluorescence. Relative to the origin of bare PQ at 29524 cm<sup>-1</sup>,<sup>21</sup> it is red-shifted by 1463 cm<sup>-1</sup>.

We also recorded an IR/UV hole-burning spectrum with the IR-laser tuned to 3411 cm<sup>-1</sup>. As will be shown in the following, this frequency corresponds to one of the vibrations measured by FDIR detecting a total yield of fluorescence with the UV laser tuned to 28061 cm<sup>-1</sup>. If all the solvent-induced spectral features in Figure 2a are from the same neutral cluster, their intensity should be equally decreased when recorded with the IR-burn laser switched on. Since this was the case (Figure 2b), we can assign these solvent-induced bands to only one solvated species, which still has to be assigned. For recording the hole-burning spectrum we used the experimental setup in Frankfurt. There it was not possible to measure the LIF spectrum above  $\approx 28300$  cm<sup>-1</sup> due to limited efficiency of the dye used. For this reason we could not extend the hole-burning spectrum beyond this energy limit.

The red-shift of the origin with respect to the location in bare PQ (1463 cm<sup>-1</sup>) can be compared with the analogous shift observed for the PQ/methanol<sub>2</sub> complex (1651 cm<sup>-1</sup>) which was unambiguously assigned by means of FDIR spectroscopy.<sup>7</sup> It should also be pointed out that the LIF spectrum disappears at excess energies above 471 cm<sup>-1</sup>, which compares well with the spectrum of the PQ/methanol<sub>2</sub> complex which is quenched beyond 663 cm<sup>-1</sup>.

**3.3. FDIR and IR/fsMPI Spectra.** The ground-state FDIR depletion spectrum measured by probing the fluorescence signal upon excitation of the band at 28061 cm<sup>-1</sup> is shown in Figure 3a. While only very weak IR activity, if at all, was detected for the region of free OH vibrations, three intense bands at 3140, 3310, and 3411 cm<sup>-1</sup> are observed corresponding to the hydrogen-bonded NH and OH stretching vibrations, significantly red-shifted in their values from those observed for the isolated molecules: 3507 cm<sup>-1</sup> for PQ,<sup>7</sup> and 3657 and 3756 cm<sup>-1</sup> for water.<sup>23</sup> Hence, the fluorescent species possesses three hydrogen bonds, indicating that at least two water molecules must be involved in the cluster responsible for the LIF spectrum. Since structurally related PQ/methanol <sub>$n=1,2$</sub>  clusters reveal IR activity in the same region,<sup>7</sup> we further concentrated on the 3100–3450 cm<sup>-1</sup> spectral part.

The IR/fsMPI spectra measured in parallel for the PQ<sup>+</sup>/water <sub>$n$</sub>  ( $n = 0, 1$ , and 2) ion channels are presented in Figure 3 (traces d, c, and b, respectively). These spectra are nearly saturated because they were taken with a tightly focused laser beam in



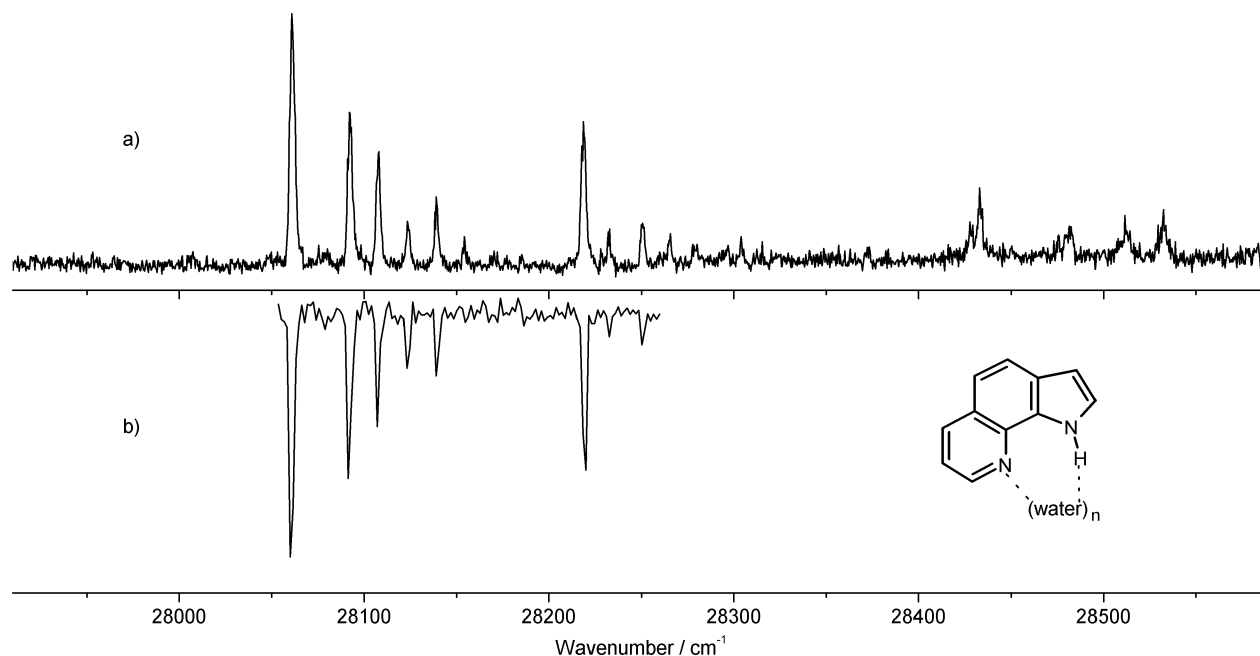


**Figure 2.** LIF excitation spectrum (a) and IR-UV hole-burning spectrum at  $3411\text{ cm}^{-1}$  (b) recorded in the region where the  $\text{PQ}/\text{water}_{n=1,2}$  clusters should exhibit spectral activity according to our calculations.<sup>5</sup>

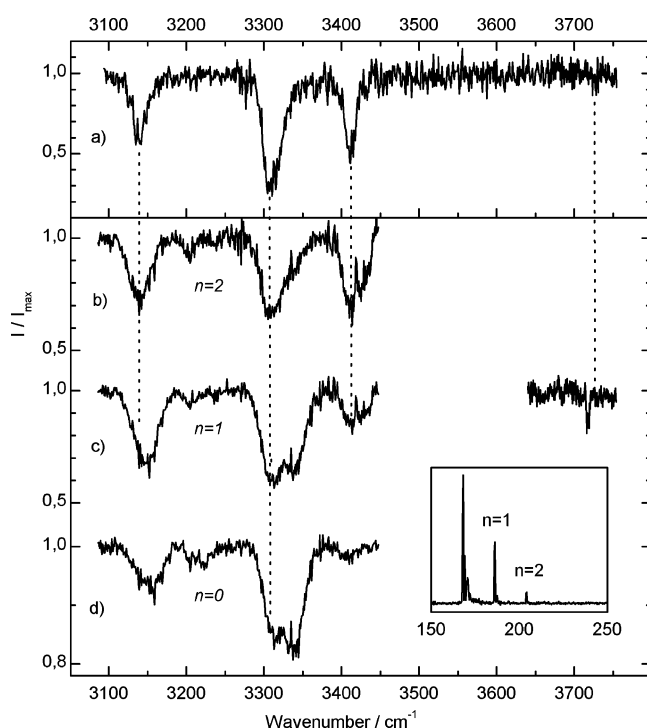


**Figure 3.** A comparison of the FDIR spectrum (a) measured upon excitation of the transition at  $28061\text{ cm}^{-1}$  with the IR/fsMPI spectra recorded in (b)  $1^{+}:2$ , (c)  $1^{+}:1$ , and (d)  $1^{+}:0$  cluster channels.<sup>22</sup> The inserted mass spectrum shows the corresponding cluster ion distribution. The dotted line above  $3700\text{ cm}^{-1}$  indicates the very weak free OH stretch, which is also very weak in the calculated spectra (Figure 5).

order to detect weaker double resonance bands. While the depletion of the fluorescence signal reached a value of 75%, significant cluster fragmentation caused the ion depletion not to exceed 40% at signal levels that were one-to-two orders of magnitude weaker than that of fluorescence. The IR/fsMPI spectrum detected for the  $\text{PQ}^{+}/\text{water}_2$  ion signal (Figure 3b) matches the above FDIR spectrum very well. Weaker additional features at  $3205$  and  $3430\text{ cm}^{-1}$  can arise from larger clusters fragmenting into this ion channel or can be due to less stable

isomers of the  $1:2$  complex. The spectra of the clusters larger than  $1:2$  were not measured due to insufficient levels of the corresponding ion signals (see the mass spectrum in Figure 3). Close similarity of the spectra depicted in Figure 3, parts a and b, proves that the smallest fluorescent complex of PQ with water contains two solvent molecules. It should be emphasized that the photoionization of the PQ clusters by femtosecond laser pulses at  $266\text{ nm}$  is not isomer-selective. It can be therefore concluded that one conformer of the PQ complex with two water molecules is dominant in all spectra under supersonic jet conditions.

The bands at  $3310$  and  $3411\text{ cm}^{-1}$  are common for the spectra of the  $1^{+}:1$  and  $1^{+}:2$  ions, thus providing evidence for the fragmentation of the heavier complex by loss of one water molecule. In the depletion spectrum of the  $1^{+}:1$  channel (Figure 3c) one band appears at  $3148\text{ cm}^{-1}$ , at a slightly different wavelength than the band at  $3140\text{ cm}^{-1}$  recorded on the  $1^{+}:2$  cluster (Figure 3b). This fact indicates two close-lying transitions of the  $1:1$  and  $1:2$  clusters which overlap in the lower mass channel. The peak at  $3341\text{ cm}^{-1}$  is observed exclusively for the  $1^{+}:1$  and the  $1^{+}:0$  channels and therefore must stem from the  $1:1$  complex. Actually, the spectrum recorded at the monomer ion channel (Figure 3d) reveals all the features found for the  $1^{+}:1$  ions, however, again with different relative intensities of the particular bands.

It was not possible to find expansion conditions under which only  $1:1$  complexes were formed. The  $1^{+}:1$  channel was contaminated by contributions from fragmenting higher clusters, manifested by the  $3310\text{ cm}^{-1}$  band always appearing in the depletion spectrum of the  $1^{+}:1$  channel. However, it was straightforward to distinguish between species belonging to different stoichiometry. For that, the spectra recorded in the  $1^{+}:1$  channel were compared for different water pressures in Figure 4. The ratio between the peaks at  $3341$  and  $3310\text{ cm}^{-1}$  increased for smaller water concentrations. At the same time, the low-energy band around  $3150\text{ cm}^{-1}$  shifted to the blue by about  $10\text{ cm}^{-1}$ ; this was accompanied by a decrease in intensity. These findings leave no doubt about the assignment of  $3341$  and  $3310\text{ cm}^{-1}$  bands to  $1:1$  and  $1:2$  stoichiometry, respectively. They

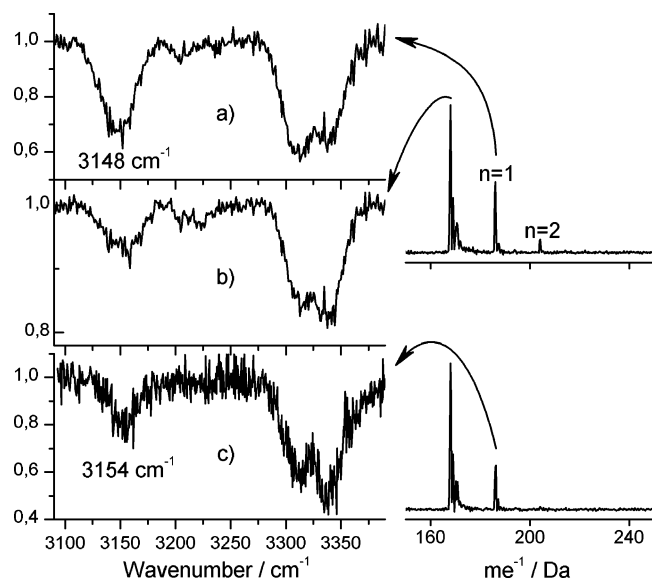


**Figure 4.** IR/fsMPI spectra measured in the  $1^+1$  (a,c) and  $1^+0$  (b) PQ/water cluster channels. Parts (a) and (c) represent different cluster distributions. The corresponding mass spectra are shown on the right.

also confirm that both types of complexes absorb at around  $3150\text{ cm}^{-1}$ , albeit with different probabilities, and that the corresponding vibrational transition in the 1:1 complex is weaker and blue-shifted with respect to that of the 1:2 species. These conclusions were firmly corroborated by comparing band intensities in the  $1^+2$ ,  $1^+1$ , and  $1^+0$  channels (Figure 3, parts b–d), with the contributions of the bands assigned to 1:1 species being stronger in the  $1^+0$  channel than that assigned to the 1:2 complex (it should be stressed that these signals were obtained simultaneously, in the same experiment).

In order to obtain a separate spectrum of the 1:1 complex alone, the depletion spectrum of the  $1^+2$  ions (Figure 3b) was subtracted from that recorded in the  $1^+1$  channel (Figure 3c). Such methodology is well-established, for example, in the analysis of linear dichroism spectra, where it is known as a “stepwise reduction procedure”.<sup>24</sup> In order for this approach to be reliable the peak positions must be separated in the two spectra. This is the case for the bands at  $3310$  and  $3341\text{ cm}^{-1}$ , but not for the bands around  $3150\text{ cm}^{-1}$ . The former two can be therefore safely separated by finding a linear combination of the spectra for which the feature at  $3310\text{ cm}^{-1}$  disappears completely. In principle, one could use the same weighting factor for the whole spectrum. However, it is quite probable that the fragmentation efficiency is vibrational-mode-dependent (for instance, mode-specific IVR/predissociation dynamics has been demonstrated for phenol dimer in the picosecond IR-UV pump–probe investigations by Ebata et al.<sup>25</sup>). For this case, a single weighting factor is not justified. We have therefore performed the subtraction using different factors for different bands. The results reveal a remarkable stability in the band frequency ( $\pm 2\text{ cm}^{-1}$ ). An additional criterion for a proper choice of the weighting coefficients is the limitation that the obtained signal should not exceed unity, since only depletion is experimentally observed. Using the above approach, one obtains a spectrum of the 1:1 complex shown in Figure 5a. We consider the band positions in the spectrum to be quite reliable, whereas the relative intensities may be uncertain; we estimate the inaccuracy of the intensity ratio to lie within  $\pm 25\%$ .

Having obtained by this analysis the vibrations of the complexes with one and two water molecules, one can determine their contributions to the depletion spectrum of the  $1^+0$  channel

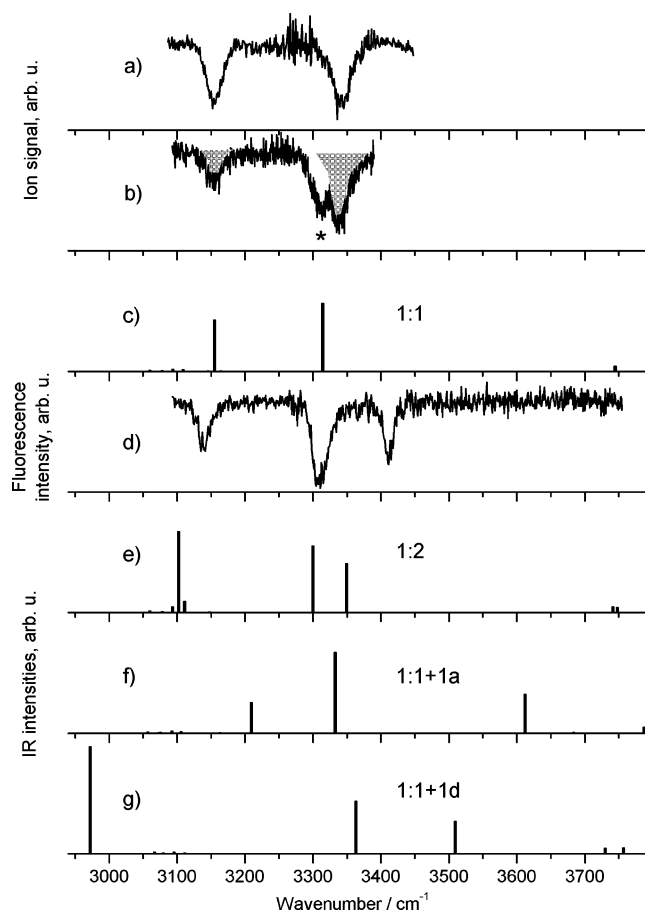


**Figure 5.** The ground-state vibrational spectra of the 1:1 (a,b) and 1:2 (d) complexes. Spectrum (a) was obtained using the subtraction procedure, and spectrum (b) was recorded directly in the  $1^+1$  channel at low water concentration. The asterisk denotes the band of the 1:2 complex caused by fragmentation. The “IR fingerprints” of the relevant clusters, calculated at the B3LYP/cc-pVDZ level of theory, are depicted by the stick spectra (c, e–g).

**TABLE 2: Relative Intensities of the Vibrational Bands Detected in the Depletion Spectra in Different Ion Channels by IR/fsMPI Spectroscopy**

| ion channel | 1:1                   |                       | 1:2                   |                       |                       |
|-------------|-----------------------|-----------------------|-----------------------|-----------------------|-----------------------|
|             | $3155\text{ cm}^{-1}$ | $3341\text{ cm}^{-1}$ | $3140\text{ cm}^{-1}$ | $3310\text{ cm}^{-1}$ | $3411\text{ cm}^{-1}$ |
| $1^+2$      |                       |                       | 0.30                  | 0.35                  | 0.35                  |
| $1^+1$      | 0.20                  | 0.20                  | 0.20                  | 0.35                  | 0.15                  |
| $1^+0$      | 0.05                  | 0.15                  | 0.05                  | 0.12                  | 0.02                  |

(Figure 3d). The relative intensities of the particular vibrations in the spectra measured in all three ion channels are summarized in Table 2. Their different values in the lower ion channels give evidence that photofragmentation efficiency depends on the mode of the vibrational preexcitation.

**3.4. Vibrational Analysis of the IR Spectra.** The vibrational spectra assigned above to the PQ/water<sub>*n*=1,2</sub> complexes and the theoretical IR “fingerprints” are compared in Figure 5. Excellent agreement of the experimental and calculated spectra of the 1:1 cluster (Figure 5, parts a–c) in the region of hydrogen-bonded NH and OH stretch vibrations provides a strong argument for the cyclic double hydrogen-bonded structure (1:1 in Figure 1) of this species. The bands at  $3341$  and  $3155\text{ cm}^{-1}$  are readily identified as simultaneous out-of-phase and in-phase stretches of the hydrogen-bonded NH and OH groups, respectively (Figure 6). The in-phase vibration may be considered as a double proton-transfer promoting mode.

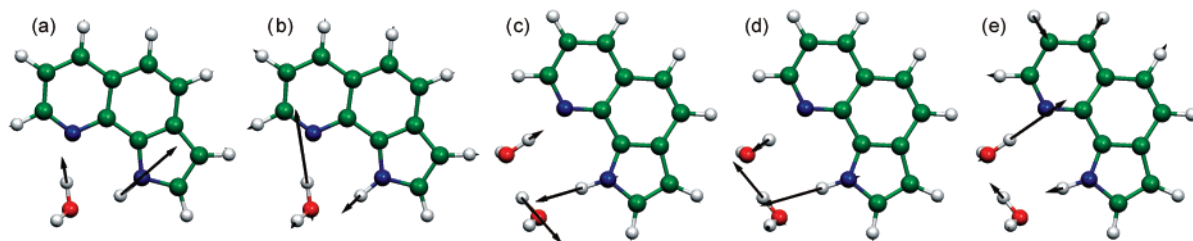


**Figure 6.** Normal modes showing hydrogen-bonded NH and OH stretching motions, calculated for the 1:1 and 1:2 PQ/water complexes: (a) 3314  $\text{cm}^{-1}$ , (b) 3155  $\text{cm}^{-1}$ , (c) 3349  $\text{cm}^{-1}$ , (d) 3300  $\text{cm}^{-1}$ , and (e) 3103  $\text{cm}^{-1}$ .

**TABLE 3: Experimental and Theoretical Frequencies of Hydrogen-Bonded NH and OH Stretch Vibrations of Selected PQ/Water Complexes**

| species | $\nu_{\text{calc}}/\text{cm}^{-1}$ | $\nu_{\text{exp}}/\text{cm}^{-1}$ | mode description   |
|---------|------------------------------------|-----------------------------------|--|
| 1:1     | 3314                               | 3341                              | out-of-phase $\text{NH}\cdots\text{O}$ and $\text{OH}\cdots\text{N}$ |
|         | 3155                               | 3155                              | "proton transfer"  |
| 1:2     | 3349                               | 3411                              | water dimer OH   |
|         | 3300                               | 3310                              | out-of-phase $\text{NH}\cdots\text{O}$ and $\text{OH}\cdots\text{N}$ |
|         | 3103                               | 3140                              | "proton transfer"  |
| 1:1+1a  | 3612                               |                                   | water dimer OH   |
|         | 3333                               |                                   | out-of-phase $\text{NH}\cdots\text{O}$ and $\text{OH}\cdots\text{N}$ |
|         | 3210                               |                                   | "proton transfer"  |
| 1:1+1d  | 3509                               |                                   | water dimer OH   |
|         | 3363                               |                                   | out-of-phase $\text{NH}\cdots\text{O}$ and $\text{OH}\cdots\text{N}$ |
|         | 2972                               |                                   | "proton transfer"  |

Of the three complexes containing two water molecules, the mode pattern calculated for the 1:2 (Figure 5e) exhibits the closest agreement with experiment (Figure 3, parts a and b). Since the spectrum in Figure 3b represents the major spectral features detected in the depletion spectrum of the  $1^+2$  channel and the minor additional features of the latter are assignable to fragmentation, we can rule out a significant amount of the additional complexes of the same stoichiometry, such as the 1:1+1a and 1:1+1d, under our experimental conditions. The calculated binding energies indicate that these clusters should be less stable by several kcal/mol relative to the 1:2 complex (Table 1). Hence, the bands at 3411, 3310, and 3140  $\text{cm}^{-1}$  are assigned to the donor OH stretch of the water dimer, the out-of-phase  $\text{NH}\cdots\text{O}$  and  $\text{OH}\cdots\text{N}$  and the in-phase "proton transfer" vibrational modes, respectively. The above assignment is summarized in Table 3. The relevant normal modes are visualized in Figure 6. Interestingly, the assignment of the 3310 and 3341  $\text{cm}^{-1}$  bands to the out-of-phase  $\text{NH}\cdots\text{O}$  and  $\text{OH}\cdots\text{N}$  modes of the 1:2 and 1:1 complexes, respectively, is corroborated by an enhanced contribution of those bands to the  $1^+0$  fragment channel (Figure 3, Table 2) reflecting the repulsive character of the concerted oscillation of the protons between the chromophore and the water bridge. By comparison of MP2 and DFT calculations, we previously demonstrated that the contribution of particular local stretches to the normal modes may significantly change depending on the level of theory.<sup>7</sup> However, their sequence frequency is not affected. The same frequency order of the stretch modes has been observed for other systems with a triple hydrogen-bonding cycle, such as 7-hydroxyquinoline/methanol.<sup>26</sup>

#### 4. Discussion

Even though the IR/fsMPI technique resembles in many aspects the hole-burning procedures, the basic difference has to be pointed out. In general, the IR/fsMPI approach is not specific with respect to stoichiometry (size), structure, or spectra. Therefore, the obtained spectra may at first look rather imperfect, since they can contain contributions from different species. Moreover, the relative contributions, even in the same channel,

may not properly reflect the IR absorption probability, since the signal may be vibrational-mode-specific. However, advantages are overwhelming. One gets a possibility to simultaneously monitor the behavior of different species present in the system, in particular the short-lived ones, which escape detection by other techniques, such as FDIR. In principle, the complicated pattern of peak intensities in various channels could also be used to trace down the pathways of dissociation.

The negative depletion signal in all ion channels suggests that vibrational excitation leads to a decrease of the UV absorption probability or to depopulation of the species, or to a combination of both. The former factor can be caused by a change of Franck–Condon overlap of the optical transition upon IR excitation. This mechanism provides the possibility to measure IR depletion spectra of covalently bound molecules, for which predissociation of subunits is energetically not possible. Noncovalently bound clusters can fragment in this way. The present IR/fsMPI spectra, dominated by fragmentation, indicate that dissociation is the main source of the signal. Depending on the binding energy and photoionization conditions, the process can occur in the ground, excited, and ionic states. As we observed only depletion signals, the fragments had enough initial energy to escape the beam. The required kinetic resource was provided by photoionization with considerable excess energy ( $2 \times 266 \text{ nm}$ ).

FDIR and IR/fsMPI measurements demonstrate that the smallest fluorescing microhydrate contributing to the LIF excitation spectrum must be assigned to the PQ/water<sub>2</sub> complex. Failure to detect the 1:1 clusters in the LIF spectrum can be due to its rapid depopulation via ESPT. This is the most reliable explanation based on solution data,<sup>1,4,27</sup> calculations,<sup>5–6</sup> and studies of jet-cooled PQ/methanol clusters.<sup>7,9</sup> Other possible mechanisms of rapid excited-state deactivation, such as inter-system crossing or enhanced internal conversion, have been discussed in numerous previous works.<sup>27–32</sup> Transient absorption spectroscopy results demonstrated that the intersystem crossing channel becomes inefficient in protic solvents.<sup>28</sup> In turn, enhanced internal conversion was found to be efficient in solvates of 1:2 stoichiometry.<sup>27,28,30</sup>

The 3341  $\text{cm}^{-1}$  band, assigned to the 1:1 complex with water, is 73  $\text{cm}^{-1}$  higher in energy than the corresponding vibration in the 1:1 complex with methanol (3268  $\text{cm}^{-1}$ ). Similarly, the 3310 and 3411  $\text{cm}^{-1}$  vibrations of the 1:2 complex with water also exhibit blue-shifts of 105 and 79  $\text{cm}^{-1}$  in comparison with the 3205 and 3332  $\text{cm}^{-1}$  bands, observed with methanol. The energy of the water dimer OH-donor vibration (3411  $\text{cm}^{-1}$ ) is shifted by  $-190 \text{ cm}^{-1}$  relative to that of the isolated water dimer (3601  $\text{cm}^{-1}$ ), as reported by Huisken et al.<sup>33</sup> The corresponding frequency reduction of the OH-donor dimer vibration in the case of the methanol 1:2 complex was found to be  $-242 \text{ cm}^{-1}$ . Since for a similar cluster structure the value of the red-shift of a donor stretch correlates with the strength of the hydrogen bond, the hydrogen bond in the 1:1 and 1:2 clusters with methanol is

stronger than with water. The above relations are in good agreement with the calculated binding energies, which are repeatedly larger for the methanol complexes (Table 1).

## 5. Conclusions

In this work, we have investigated the structure of isolated PQ/water<sub>*n*</sub> (*n* = 1,2) complexes. By combining the IR/fsMPI and FDIR spectroscopies in the region of hydrogen-bonded NH and OH stretch vibrations with DFT calculations, we detected two different complexes of PQ with water. The structures of the 1:1 and 1:2 clusters were assigned to cyclic doubly and triply hydrogen-bonded species, respectively (Figure 1), similar to the analogous system with methanol. The photofragmentation efficiency of the clusters in the applied IR/fsMPI scheme was found to be affected by vibrational preexcitation, depending on the vibrational mode. Both 1:1 and 1:2 complexes of PQ with water reveal weaker hydrogen bonding than those with methanol.

**Acknowledgment.** We dedicate this work to the memory of Roger E. Miller, a true pioneer of cluster spectroscopy, who stimulated us by his seminal scientific contributions to this field. Y.N. acknowledges support from the EC Grant G5MA-CT-2002-04026. C.R. acknowledges gratefully the Adolf-Messer-Stiftung, the friends and promoters of the University of Frankfurt/Main, and the DFG. R.P.T. thanks the Robert A. Welch Foundation and the NSF for financial support. B.B. thanks the DFG for funding by the German-French binational research program.

## References and Notes

- (1) Kyrychenko, A.; Herbich, J.; Izydorzak, M.; Wu, F.; Thummel, R. P.; Waluk, J. *J. Am. Chem. Soc.* **1999**, *121*, 11179–11188.
- (2) del Valle, J. C.; Domínguez, E.; Kasha, M. *J. Phys. Chem. A* **1999**, *103*, 2467–2475.
- (3) Kijak, M.; Zielińska, A.; Thummel, R. P.; Herbich, J.; Waluk, J. *Chem. Phys. Lett.* **2002**, *366*, 329–335.
- (4) Marks, D.; Zhang, H.; Borowicz, P.; Waluk, J.; Glasbeek, M. J. *Phys. Chem. A* **2000**, *104*, 7167–7175.
- (5) Kyrychenko, A.; Waluk, J. *J. Phys. Chem. A* **2006**, *110*, 11958–11967.
- (6) Kyrychenko, A.; Stepanenko, Y.; Waluk, J. *J. Phys. Chem. A* **2000**, *104*, 9542–9555.
- (7) Nosenko, Y.; Kyrychenko, A.; Thummel, R. P.; Waluk, J.; Brutschy, B.; Herbich, J. *Phys. Chem. Chem. Phys.* **2007**, *9*, 3276–3285.
- (8) (a) Page, R. H.; Shen, Y. R.; Lee, Y. T. *J. Chem. Phys.* **1988**, *88*, 4621–4636. (b) Riehn, C.; Lahmann, C.; Wassermann, B.; Brutschy, B. *Chem. Phys. Lett.* **1992**, *197*, 443–450. (c) Tanabe, S.; Ebata, T.; Fujii, M.; Mikami, N. *Chem. Phys. Lett.* **1993**, *215*, 347–352. (d) Pribble, R. N.; Zwier, T. S. *Science* **1994**, *265*, 75–79.
- (9) Nosenko, Y.; Kunitski, M.; Thummel, R. P.; Kyrychenko, A.; Herbich, J.; Waluk, J.; Riehn, C.; Brutschy, B. *J. Am. Chem. Soc.* **2006**, *128*, 10000–10001.
- (10) Wu, F.; Chamchoumis, C. M.; Thummel, R. P. *Inorg. Chem.* **2000**, *39*, 584–590.
- (11) (a) Walther, Th.; Bitto, H.; Minton, T. K.; Huber, J. R. *Chem. Phys. Lett.* **1994**, *231*, 64–69. (b) Ebata, T.; Mizuochi, N.; Watanabe, T.; Mikami, N. *J. Chem. Phys.* **1996**, *100*, 546–550.
- (12) Brutschy, B. *Chem. Rev.* **2000**, *100*, 3891–3920.
- (13) Weichert, A.; Riehn, C.; Barth, H.-D.; Lembach, G.; Zimmermann, M.; Brutschy, B.; Podenas, D. *Rev. Sci. Instrum.* **2001**, *72*, 2697–2708.
- (14) Krauss, O.; Brutschy, B. *Chem. Phys. Lett.* **2001**, *350*, 427–433.
- (15) Lias, S. G.; Bartmess, J. E.; Liedman, J. F.; Holmes, J. L.; Levin, R. D.; Mallard, W. G. *J. Phys. Chem. Ref. Data* **1988**, *17*, Suppl. 1.
- (16) Taft, R. W.; Koppel, I. A.; Topsom, R. D.; Anvia, F. J. *Am. Chem. Soc.* **1990**, *112*, 2047–2052.
- (17) Lee, H. M.; Suh, S. B.; Lee, J. Y.; Tarakeshwar, P.; Kim, K. S. *J. Chem. Phys.* **2000**, *112*, 9759–9772.
- (18) Hagemester, F. C.; Gruenloh, C. J.; Zwier, T. S. *Phys. Chem. A* **1998**, *102*, 82–94.
- (19) Ahlrichs, R.; Bär, M.; Häser, M.; Hom, H.; Kölmel, C. *Chem. Phys. Lett.* **1989**, *162*, 165–169.
- (20) Witek, H. A.; Morokuma, K. *J. Comput. Chem.* **2004**, *25*, 1858–1864.
- (21) Krauss, O. Ph.D. Thesis, Goethe University, Frankfurt/M, Germany, 2002.
- (22) The IR/fsMPI spectra have been recorded in a somewhat smaller range than the FDIR spectrum. This was due to technical problems, such as significantly reduced IR intensity within 3450–3500 cm<sup>-1</sup> and thermal pointing instability of the femtosecond laser system, which allowed only a limited scanning range without readjustment. Due to the great similarity of the absorption bands observed in the IR/fsMPI and FDIR spectra (Figure 3, parts a and b), the former was recorded only up to 3450 cm<sup>-1</sup>.
- (23) Herzberg, G. *Molecular Spectra and Molecular Structure*; Van Nostrand Reinhold: New York, 1945; Vol. 2.
- (24) Thulstrup, E. W.; Michl, J. *J. Am. Chem. Soc.* **1982**, *104*, 5594–5604.
- (25) Ebata, T.; Kayano, M.; Sato, S.; Mikami, N. *J. Phys. Chem. A* **2001**, *105*, 8623–8628.
- (26) Matsumoto, Y.; Ebata, T.; Mikami, N. *J. Phys. Chem. A* **2002**, *106*, 5591–5599.
- (27) Waluk, J. *Acc. Chem. Res.* **2003**, *36*, 832–838.
- (28) Herbich, J.; Hung, C. Y.; Thummel, R. P.; Waluk, J. *J. Am. Chem. Soc.* **1996**, *118*, 3508–3518.
- (29) Dobkowski, J.; Herbich, J.; Galievsky, V.; Thummel, R. P.; Wu, F. Y.; Waluk, J. *Ber. Bunsen-Ges. Phys. Chem.* **1998**, *102*, 469–475.
- (30) Kyrychenko, A.; Herbich, J.; Wu, F.; Thummel, R. P.; Waluk, J. *J. Am. Chem. Soc.* **2000**, *122*, 2818–2827.
- (31) Herbich, J.; Waluk, J.; Thummel, R. P.; Hung, C. Y. *Photochem. Photobiol. A: Chem.* **1994**, *80*, 157–160.
- (32) Herbich, J.; Rettig, W.; Thummel, R. P.; Waluk, J. *Chem. Phys. Lett.* **1992**, *195*, 556–562.
- (33) Huisken, F.; Kaloudis, M.; Kulcke, A. *J. Chem. Phys.* **1996**, *104*, 17–25.